Electronic Supplementary Material (ESI) for Journal of Materials Chemistry A.

Electronic Supplementary Information

Nanoarchitecture of MOF-Derived Nanoporous Functional Composites for Hybrid Supercapacitors

Jeonghun Kim[a,†], Christine Young[b,†], Jaewoo Lee[a], Yoon-Uk Heo[c], Min-Sik Park[d], Md. Shahriar A Hossain,[a] Yusuke Yamauchi[a,b,*] and Jung Ho Kim[a,e,*]

[a] Institute for Superconducting and Electronic Materials (ISEM), Australian Institute for Innovative Materials (AIIM), University of Wollongong, North Wollongong, NSW 2500,Australia

[b] International Center for Materials Nanoarchitectonics (MANA), National Institute for Materials Science (NIMS), 1-1 Namiki, Tsukuba, Ibaraki 305-0044, Japan

[c] Graduate Institute of Ferrous Technology (GIFT), Pohang University of Science and Technology (POSTECH), San 31, Hyoja-Dong, Pohang 790-784, Republic of Korea

[d] Department of Advanced Materials Engineering for Information and Electronics, Kyung Hee University, 1732 Deogyeong-daero, Giheung-gu, Yongin-si, Gyeonggi-do, 17104, Republic of Korea

[e] Department of Chemistry, Shanghai Key Laboratory of Molecular Catalysis and Innovative Materials, Laboratory of Advanced Materials, iChEM (Collaborative Innovation Center of Chemistry for Energy Materials), Fudan University, Shanghai 200433, China

† These authors contributed equally to this work.

* Corresponding authors: Yusuke Yamauchi and Jung Ho Kim

Email: yusuke@uow.edu.au; E-mail: jhk@uow.edu.au

Table S1. Nanoporous characteristics of prepared materials.

Samples	Specific surface area (S_{BET}, $m^2 \cdot g^{-1}$) [a]	Micropore surface area (S_{micro}, $m^2\ g^{-1}$)[b]	S_{micro}/S_{BET} (%)	Total pore volume (V_{pore}, $cm^3\ g^{-1}$) [b]	Micropore volume ($V_{micropore}$, $cm^3\ g^{-1}$) [b]	$V_{micropore}$ /V_{pore} (%)
HZ	1481	1466	98.9	0.62	0.57	91.9
HZ-NPC	298.24	249.01	83.5	0.4235	0.3471	81.9
HZ-NPFC/250-2	223.46	202	90	0.5023	0.3050	60.7
HZ-NPFC/250-5	202.02	184	91	0.6381	0.4685	73.4
HZ-NPFC/300-2	32.093	NA	NA	0.3506	NA	NA
HZ-NPFC/300-5	21.1	NA	NA	0.1866	NA	NA

a) Brunauer-Emmett-Teller (BET) method; b) t-plot method

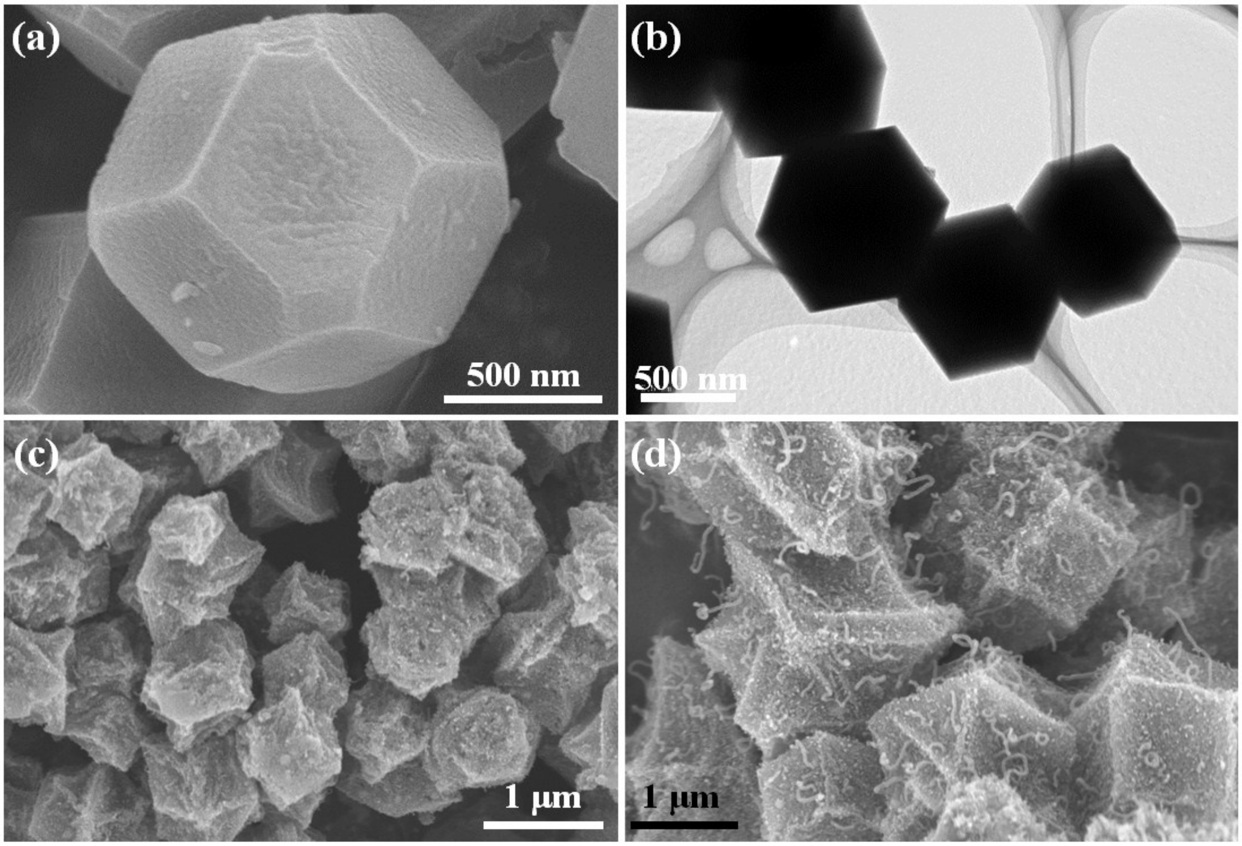

Figure S1. (a) SEM and (b) TEM images of HZ, respectively. SEM images of HZ-NPC carbonized at 800 °C according to different temperature ramp rates: (c) 5 °C min^{-1} and (d) 2 °C min^{-1}.

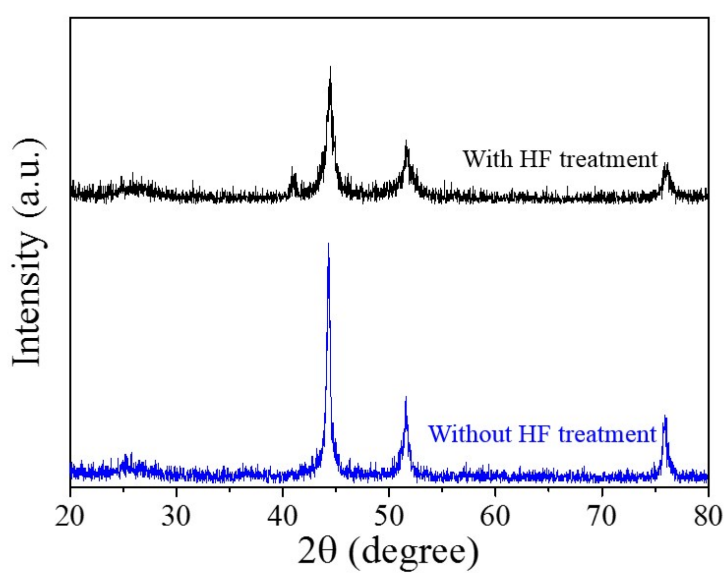

Figure S2. Wide-angle XRD patterns of HZ-NPC with (upper) and without (lower) an HF(aq) washing treatment.

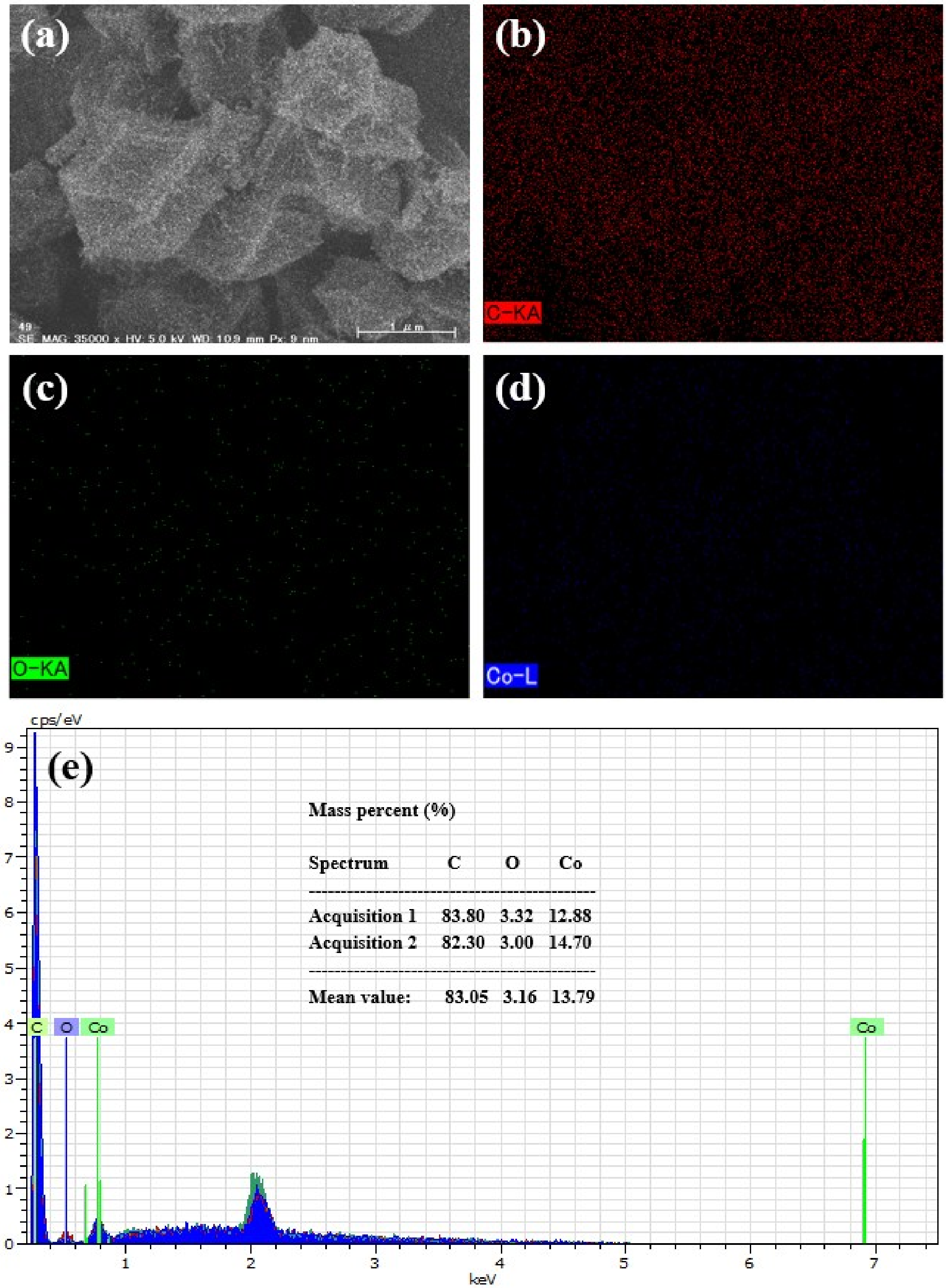

Figure S3. (a) SEM image, (b-d) EDS mapping and (e) EDS spectrum for element (C, O, and Co) analysis of carbonized HZ-NPC at 800 °C with HF(aq) washing.

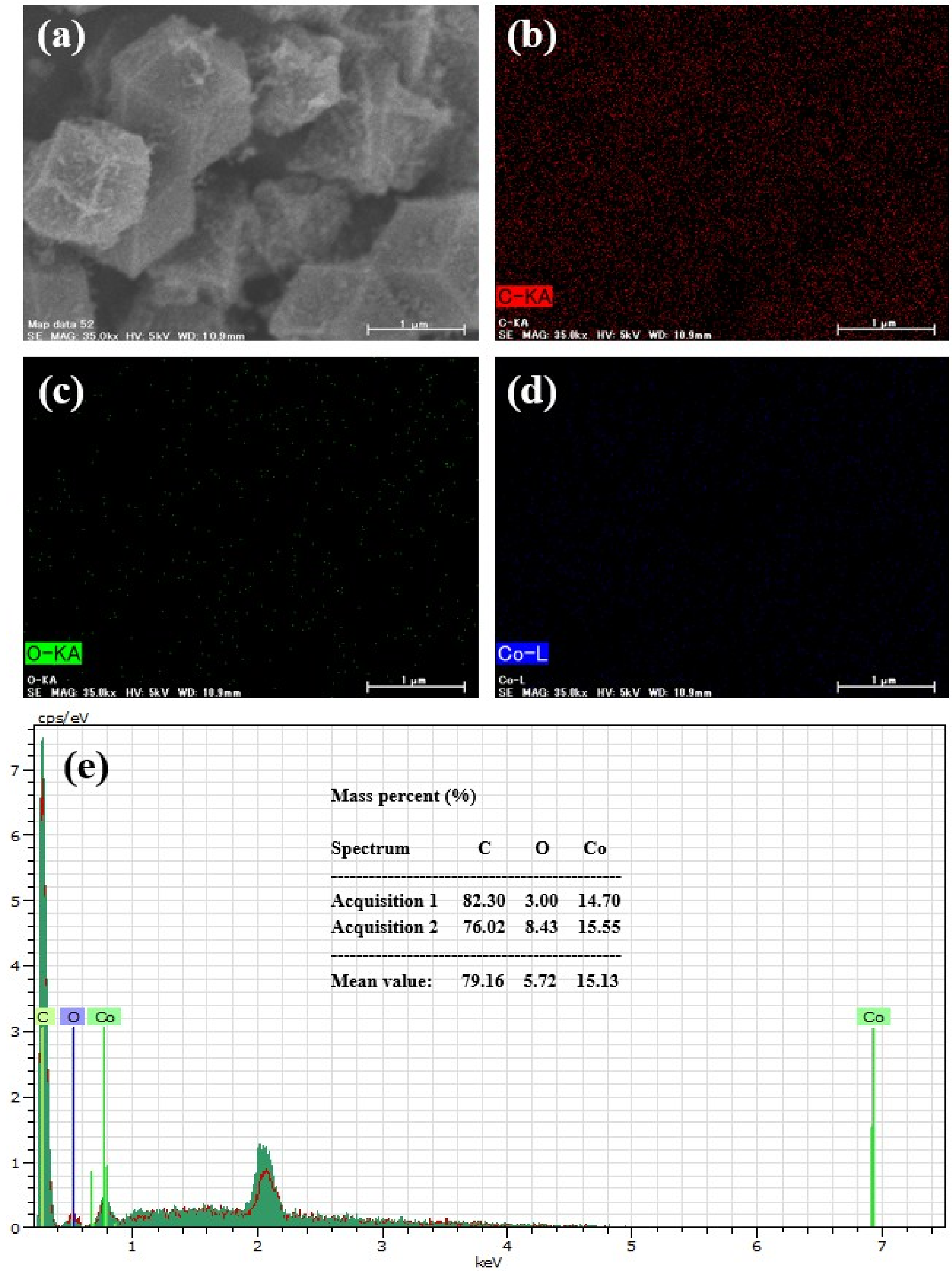

Figure S4. (a) SEM image, (b-d) EDS mapping and (e) EDS spectrum for element (C, O, and Co) analysis of carbonized HZ-NPC at 800 °C without HF(aq) washing.

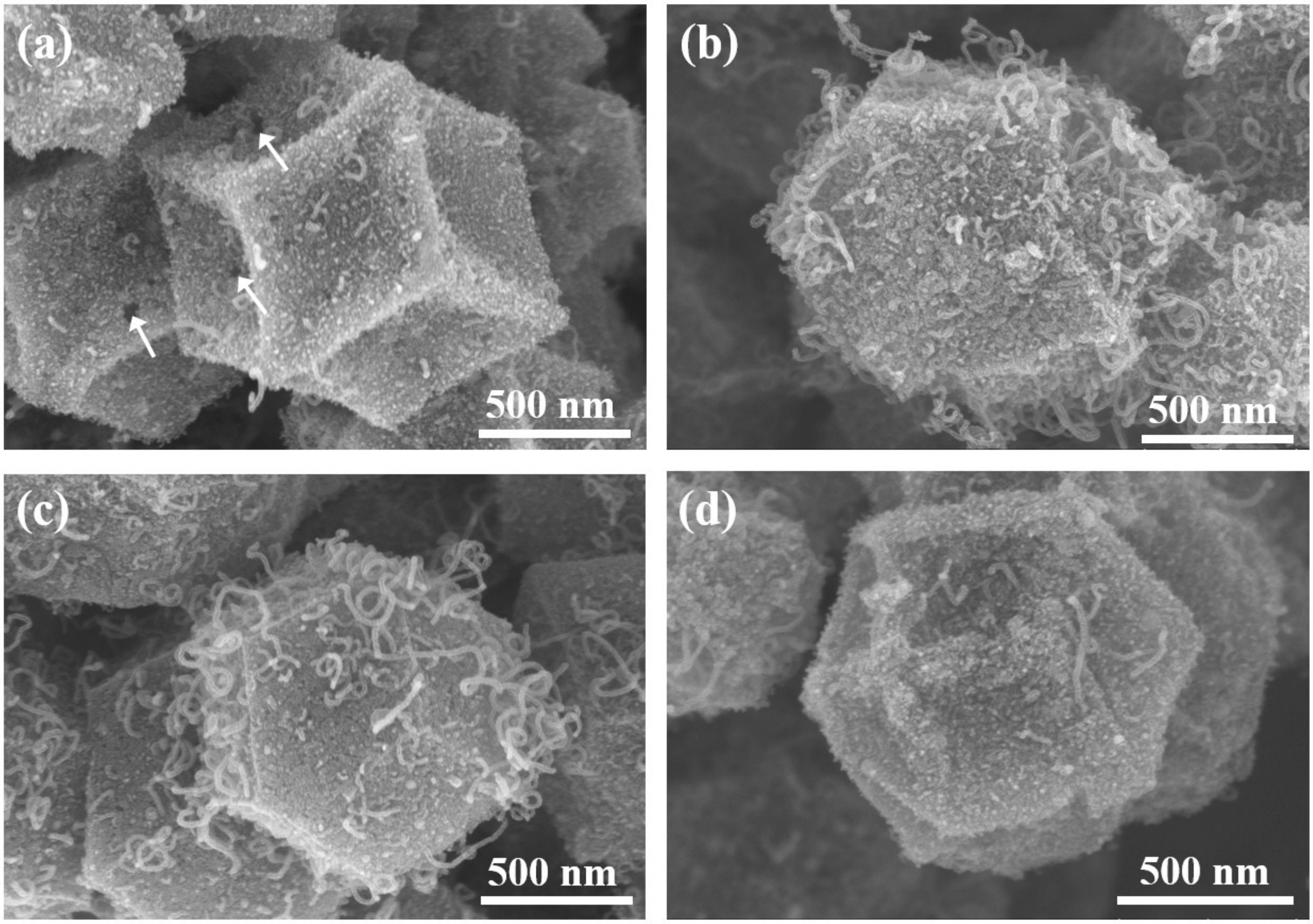

Figure S5. SEM images of HZ-NPCs with (a) and without (c) HF(aq) washing treatment, and (b) and (d) their corresponding HZ-NPFC/250-2 samples after oxidation at 250 °C for 2 h, respectively.

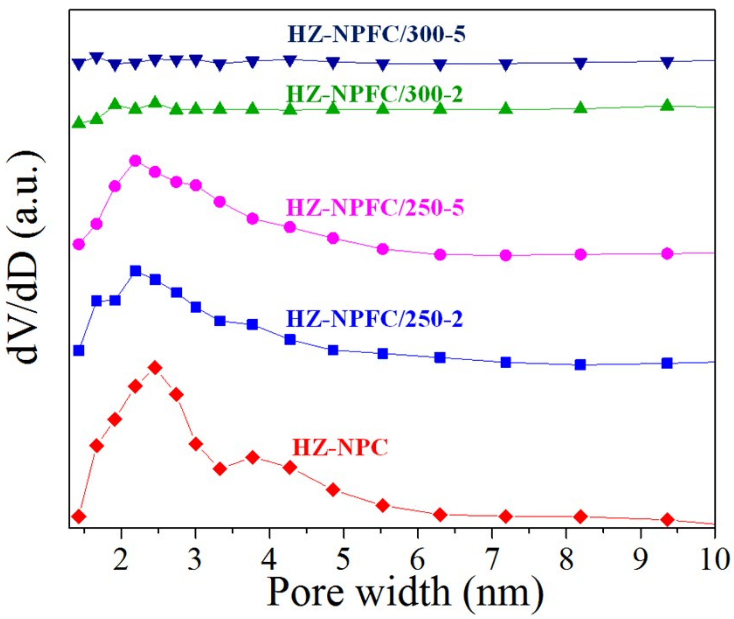

Figure S6. Pore size distributions for HZ-NPC and HZ-NPFCs in range of 1.5- 10 nm.

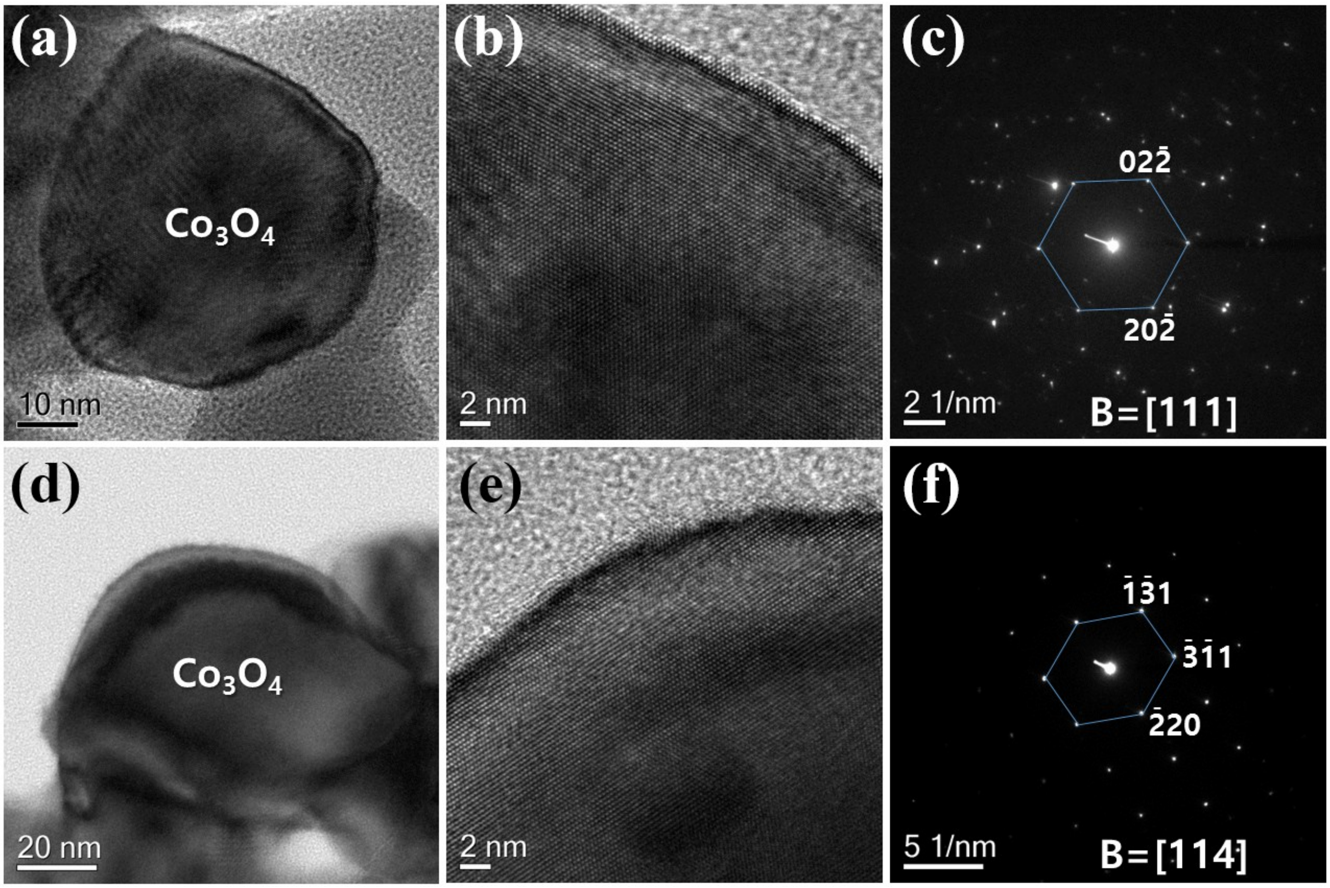

Figure S7. High resolution transmission electron microscope (HRTEM) images and corresponding fast Fourier transform (FFT) patterns of Co_3O_4 particles in (a-c) HZ-NPFC/300-2 and (d-f) HZ-NPFC/300-5.

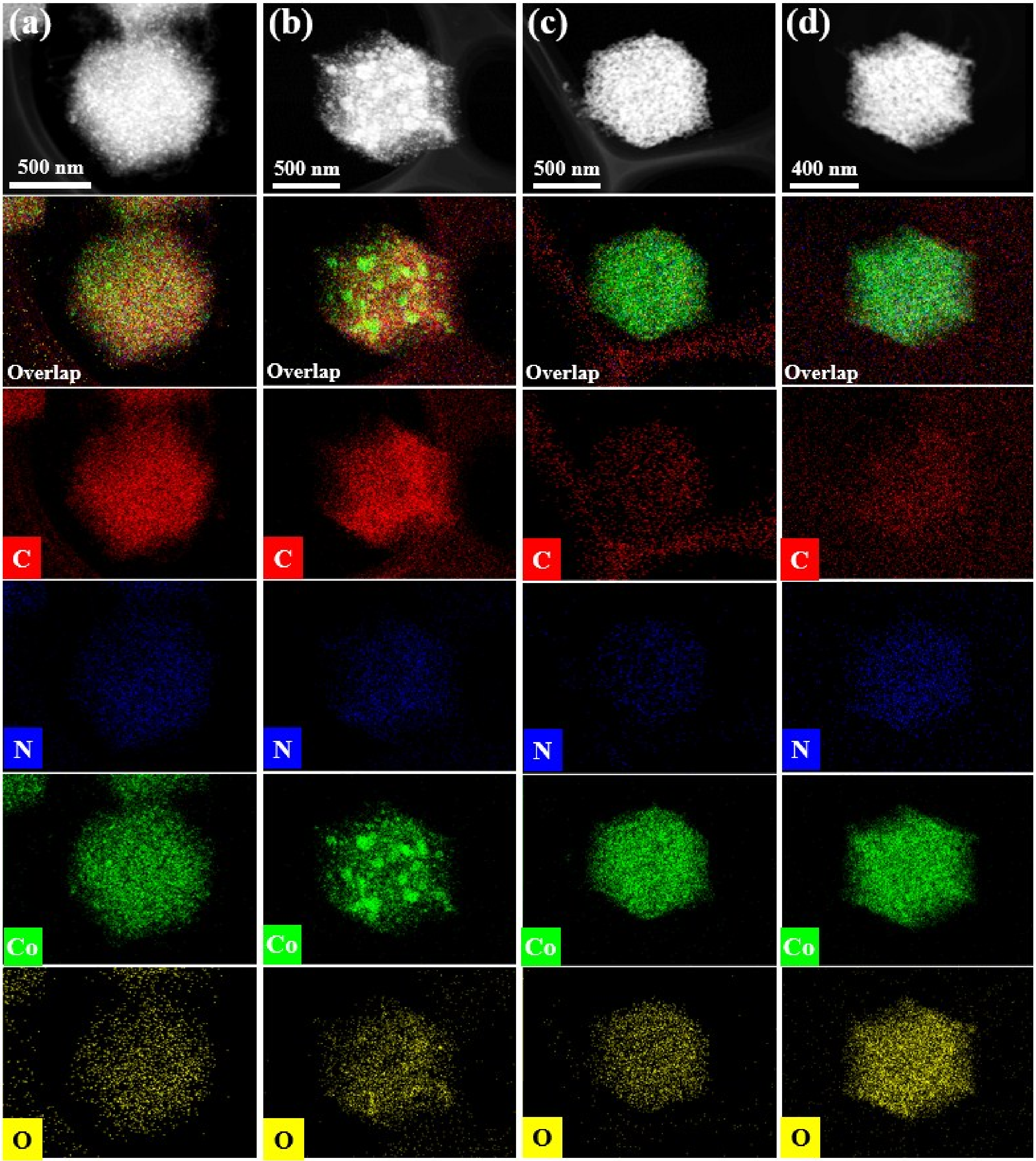

Figure S8. High-angle annular dark field-scanning TEM (HAADF-STEM) images and EDS mapping of (a) HZ-NPC, (b) HZ-NPFC/250-2, (c) HZ-NPFC/300-2, and (d) HZ-NPFC/300-5.

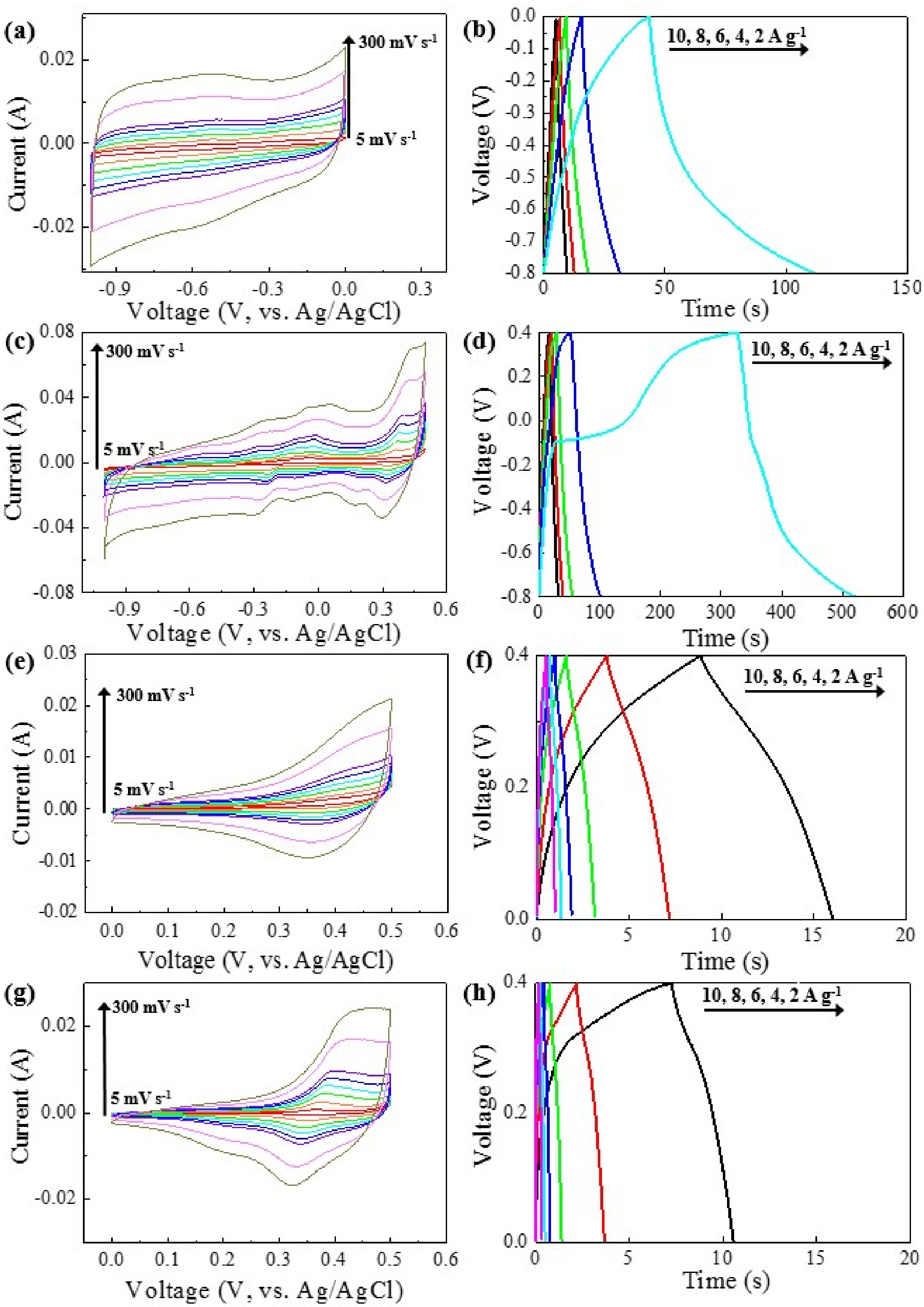

Figure S9. Cyclic voltammograms (CVs) at different scan rates (left) and galvanostatic charge-discharge curves (right) at different current densities of (a-b) HZ-NPC, (c-d) HZ-NPFC/250-2, (e-f) HZ-NPFC/300-2, and (g-h) HZ-NPFC/300-5.

Table S2. Comparison of electrochemical performance in aqueous electrolyte of HZ-NPFC/250-5 with the literature reports of zeolitic imidazolate framework (ZIF)-derived materials

Material (used metal for ZIF)	**Resulting material**	**Capacitor Type**	**Capacitance**	**Ref.**
[a] ZIF-8 (Zn)	N-doped nanoporous carbon	EDLC	252 $F \cdot g^{-1}$ at 5 $mV \cdot s^{-1}$	58
[a] ZIF-8 (Zn)	N-doped nanoporous carbon	EDLC	214 $F \cdot g^{-1}$ at 5 $mV \cdot s^{-1}$	34
[a] ZIF-8 (Zn)	N-doped nanoporous carbon	EDLC	219 $F \cdot g^{-1}$ at 5 $mV \cdot s^{-1}$	36
[a] ZIF-8 (Zn)	Activated high surface area N-doped nanoporous carbon	EDLC	211 $F \cdot g^{-1}$ at 10 $mV \cdot s^{-1}$	59
[a,b] Electrospun ZIF-8 (Zn)	N-doped nanoporous carbon in carbon fiber	EDLC	283.2 $F \cdot g^{-1}$ at 2 $A \cdot g^{-1}$	60
[a] ZIF-67 (Co)	N-doped nanoporous carbon	EDLC	238 $F \cdot g^{-1}$ at 20 $mV \cdot s^{-1}$	53
[a] ZIF-67 (Co)	N-doped nanoporous carbon	EDLC	272 $F \cdot g^{-1}$ at 5 $mV \cdot s^{-1}$	37
[a] ZIF-67 (Co)	Porous Co_3O_4	Pseudocapacitor	504 $F \cdot g^{-1}$ at 5 $mV \cdot s^{-1}$	37
[a] ZIF-67 (Co)	Co/ nanoporous carbon	Pseudocapacitor	160 $F \cdot g^{-1}$ at 2 $A \cdot g^{-1}$	61
[a] Hybrid ZIF (Zn, Co)	N-doped nanoporous carbon	EDLC	93 $F \cdot cm^{-3}$ at 20 $mV \cdot s^{-1}$	47
[a] Hybrid ZIF (Zn, Co)	N-doped nanoporous carbon/MWCNT/Co NP	EDLC	171 $F \cdot g^{-1}$ at 2 $A \cdot g^{-1}$	our work
[a] Hybrid ZIF (Zn, Co)	N-doped nanoporous carbon/MWCNT/Co NP/Co_3O_4	EDLC & Pseudocapacitor	545 $F \cdot g^{-1}$ at 2 $A \cdot g^{-1}$	our work
[c] ZIF-67 (Co) on Ni foam	Porous Co_3O_4 on Ni foam	Pseudocapacitor	1433 $F \cdot g^{-1}$ at 2 $A \cdot g^{-1}$	62
[c] ZIF-67 (Co) on Ni foam	Ni foam/Co/carbon	Pseudocapacitor	500.6 $F \cdot g^{-1}$ at 2 $A \cdot g^{-1}$	63
[c] ZIF-67 (Co) on carbon cloth	carbon cloth@Co_3O_4	Pseudocapacitor	900 $F \cdot g^{-1}$ at 10 $A \cdot g^{-1}$	64
[c] ZIF-67 (Co) on carbon cloth	carbon cloth@ N-doped nanoporous carbon	EDLC	321.9 at 6.25 $A \cdot g^{-1}$	64

[a] Synthesized as a single particle; [b] Embedded in polymer matrix; [c] Synthesized on electrodes.